1992ApJ...392L..83U

THE ASTROPHYSICAL JOURNAL, 392:L83–L86, 1992 June 20
© 1992. The American Astronomical Society. All rights reserved. Printed in U.S.A.

# THE OUTFLOW IN THE L1157 DARK CLOUD: EVIDENCE FOR SHOCK HEATING OF THE INTERACTING GAS[1]

T. UMEMOTO,[2] T. IWATA,[3] Y. FUKUI,[4] H. MIKAMI,[4] S. YAMAMOTO,[4] O. KAMEYA,[2] AND N. HIRANO[2]
*Received 1991 December 18; accepted 1992 April 2*

## ABSTRACT

In the L1157 dark cloud, we have discovered a well-collimated bipolar CO outflow associated with a cold *IRAS* source 20386+6751. The gas kinetic temperature toward the blue lobe of the outflow rises to ~30 K from the temperature of the surrounding gas (≤10 K); this high temperature region is very localized within the blue lobe. The $HCO^+$, HCN, and $NH_3$ lines show blueshifted and broad-line profiles toward the blue CO lobe. Furthermore, their distributions are similar to that of the blue lobe. Analysis of the energy of the outflow and dense gas suggests that a strong shock caused by the outflow is responsible for the temperature enhancement. Such shock heating has rarely been observed in low-mass star-forming regions. Our data show that the outflow has an influence on the thermal properties of the parent cloud at least locally through shock processes in its early evolutionary stage.

*Subject headings:* ISM: molecules — ISM: individual (L1157) — ISM: jets and outflows — stars: formation — shock waves

## 1. INTRODUCTION

Molecular outflows have a profound influence on structure and dynamics of the ambient molecular clouds because of their large momenta and energies (e.g., Margulis, Lada, & Snell 1989; Fukui 1989; Mizuno et al. 1990; Umemoto et al. 1991). Myers et al. (1988) found that cores with outflows have larger line widths than cores without outflows, and they suggested that the outflows are responsible for the broadening of line widths in dense cores. On the other hand, it was found from CO observations that the gas kinetic temperature of molecular outflows is equal to or lower than that of the ambient molecular gas (e.g., Lada 1985). This suggests that the postshock gas of the outflow is very rapidly cooled by radiation, and therefore molecular outflows have scarcely been considered to influence ambient clouds *thermally*. However, a few observational examples for temperature enhancement in outflows and their surroundings have been found recently. The near-infrared $H_2$ emission observed toward several energetic outflows indicates the presence of a high-temperature (~2000 K) gas component (e.g., Lane & Bally 1986), although this is only a small fraction of the total outflow mass. Observations of high-velocity $NH_3$ emission toward the outflow in the *massive* star-forming region NGC 2071 revealed that the kinetic temperature of outflowing gas is much hotter than that for the ambient cloud (Takano et al. 1985). Extended far-infrared emission from dust found in the L1551 bipolar outflow suggests radiative heating of dust by UV radiation from shocked regions of the outflow, and the mass of the corresponding gas is comparable to that of the outflow (Clark et al. 1986; Edwards et al. 1986).

Molecular outflows are frequently associated with cold and luminous *IRAS* sources (Fukui et al. 1989; Margulis, Lada, & Young 1989). Therefore we have started the molecular outflow survey toward cold *IRAS* sources in dark clouds (Fukui 1989). An infrared source IRAS 20386+6751 in the L1157 dark cloud (a distance of 440 pc; Viotti 1969) has the second coldest dust-color temperature in our survey sample. Judging from its low luminosity of 11 $L_\odot$, this is a site of low-mass star formation. In this *Letter*, we present the discovery of a bipolar outflow associated with this *IRAS* source and direct evidence for shock heating of the outflow in L1157. Such heating has rarely been observed in *low-mass* star-forming regions.

## 2. OBSERVATIONS

Observations of the $J = 1$–0 lines of CO, $HCO^+$, and HCN were simultaneously carried out in 1989 February and March with the NRO 45 m telescope. The telescope had a beam size of 17″ with a main-beam efficiency of 0.45 at 115 GHz, and a beam size of 22″ with a main-beam efficiency of 0.65 at 89 GHz. We used two cooled Schottky mixer receivers, which provided SSB system noise temperatures of 900 K at 115 GHz and 850 K at 89 GHz. The region around the *IRAS* source was mapped with a grid spacing of 20″, while the outer region was mapped with 40″ spacing. Additional one-point observations of the $J = 1$–0 lines of $^{13}CO$ and $C^{18}O$ were carried out in 1990 February, and the system noise temperature was 700 K. The $NH_3$ $(J, K) = (1, 1)$, (2, 2), and (3, 3) emission lines were observed toward three positions in 1990 March by using a cooled HEMT receiver, whose system noise temperature was 150–200 K. The beam size and beam efficiency at 23.7 GHz were 80″ and 0.8, respectively. The pointing accuracy was better than 5″ as determined by observing the SiO maser source T Cep. Observed points are illustrated in Figure 1. For all observations, we used acousto-optical spectrometers (AOSs) with 37 kHz resolution, which corresponds to velocity resolution of 0.10 km $s^{-1}$, 0.12 km $s^{-1}$, and 0.50 km $s^{-1}$ at 110 GHz, 89 GHz, and 22 GHz, respectively. AOSs were frequency-calibrated, and an uncertainty of each channel was less than 20 kHz. Typical rms noise fluctuations in the CO, $HCO^+$, HCN, $^{13}CO$, $C^{18}O$, and $NH_3$ observations were 0.7, 0.4, 0.4, 0.2, 0.2, and 0.04 K, respectively.

[1] Based on the observations made at the Nobeyama Radio Observatory (NRO). NRO is a branch of the National Astronomical Observatory, an inter-university research institute operated by the Ministry of Education, Science, and Culture, Japan.

[2] Nobeyama Radio Observatory, National Astronomical Observatory, Nobeyama, Minamisaku, Nagano 384-13, Japan.

[3] Kashima Space Research Center, Communications Research Laboratory, Kashima-machi, Ibaraki 314, Japan.

[4] Department of Astrophysics, Nagoya University, Chikusa-ku, Nagoya 464-01, Japan.



© American Astronomical Society • Provided by the NASA Astrophysics Data System

1992ApJ...392L..83U



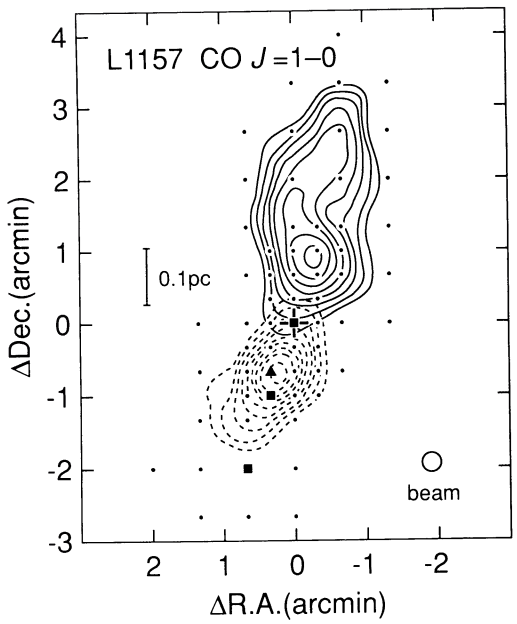


FIG. 1.—A contour map of the high-velocity CO emission in L1157. The velocity range for the blue wing (*dashed line*) is $-5.0$ to 1.0 km s$^{-1}$ and that for the red wing (*solid line*) is 4.5 to 10.5 km s$^{-1}$. Contours are every 0.9 K km s$^{-1}$ with the lowest contour at 2.7 K km s$^{-1}$. The offset center is the IRAS 20386+6751 position indicated by a cross, which corresponds to R.A.(1950) = 20$^h$38$^m$39$^s$.6, decl.(1950) = 67°51′33″. Dots denote the observed points. A filled triangle and filled squares denote the observed points by $^{13}$CO ($C^{18}O$) and $NH_3$, respectively.

## 3. RESULTS

### 3.1. CO *Molecular Outflow*

We found high-velocity CO emission around IRAS 20386+6751. The full width of CO emission is 25 km s$^{-1}$ at a 1 $\sigma$ noise level. The distribution of the redshifted and blueshifted CO emission (Fig. 1) shows a clearly defined bipolar structure centered on IRAS 20386+6751. This suggests that the *IRAS* source is the driving source of the bipolar outflow. The outflow is well collimated and elongated along the north-south direction (position angle $\sim$155°). The red lobe has a maximum extent of 0.43 pc and a width of 0.16 pc at the half-intensity level, while the blue lobe has an extent of 0.20 pc and a width of 0.12 pc. From the spatial extent and terminal velocity of the CO outflow, the dynamical time scale was estimated to be (2–3) $\times$ 10$^4$ yr.

To estimate the mass of the outflow, we should obtain the data of the optically thin line. Since we did not detect the $^{13}$CO wing with sufficient signal-to-noise ratio, the optical depth of the CO wing emission was assumed to be thin. We also assumed local thermodynamic equilibrium condition with an excitation temperature of 30 K (see § 3.3) and an abundance ratio of $[H_2]/[CO]$ of 1 $\times$ 10$^4$. Physical parameters of the outflow were calculated by the method of Iwata, Fukui, & Ogawa (1988). Results are listed in Table 1.

### 3.2. *Broad Line Emission toward the Outflow*

Figure 2 shows some molecular line spectra in the blue lobe of the CO outflow. The $HCO^+$, HCN, and $NH_3$ spectra have pedestal and blueshifted features, where the velocity of the quiescent gas is $\sim$2.7 km s$^{-1}$ which is derived from the $^{13}$CO observations. It is surprising that the line widths of $HCO^+$, HCN, and $NH_3$ are as broad as that of CO. The full velocity extent is 4 km s$^{-1}$ for $HCO^+$, $\sim$7 km s$^{-1}$ for HCN, and $\sim$10 km s$^{-1}$ for $NH_3$ (3, 3) at a 1 $\sigma$ noise level. Blueshifted and broad-line emission is also seen in SiO and CS (Mikami et al. 1992, hereafter Paper II). It is noted that the $^{13}$CO and $C^{18}O$ spectra show neither such a strong wing component nor a velocity shift. These results may indicate that there exist small dense clumps that are moving almost at outflow velocity. From CO observations, the column density at the blue lobe was estimated to be $\sim 4 \times 10^{20}$ cm$^{-2}$. If the gas density of clump is 4 $\times$ 10$^5$ cm$^{-3}$ (from LVG model for CS; Paper II), the size of clump is estimated to be smaller than 1″. Although the size itself may have a large uncertainty, it seems certain that there exits the clumpy structure smaller than the beam size. In addition, the strong $HCO^+$, HCN, $NH_3$, and SiO emission lines may suggest that the abundances of these molecules are significantly enhanced in the dense clumps.

The broad line profile is not seen at the *IRAS* source position and the red lobe. Integrated intensity map of $HCO^+$ is also shown in Figure 3. Its distribution is in alignment with the CO outflow, and shows a similar extent to that of the blue lobe. The peak position in the integrated intensity of $HCO^+$ does not correspond to the infrared source but is near the intensity maximum of the blue lobe of the outflow. The distribution of HCN also resembles that of the blue CO lobe, although it has a peak at the south end of the lobe (to be published later).

### 3.3. *Enhancement of the Gas Temperature*

Figure 3 also shows a contour map of the CO line peak intensity $T_R^*$. There is a portion where the CO intensity is significantly stronger than that of the surrounding region: the extent of the temperature-enhanced region ($\geq$8 K) well coin-

TABLE 1

PHYSICAL PARAMETERS OF THE L1157 OUTFLOW

| Component | $V_{max}$[a] (km s$^{-1}$) | Size[b] (pc) | Dynamical Time Scale[c] (yr) | Mass[d] ($M_\odot$) | Momentum[e] ($M_\odot$ km s$^{-1}$) | Energy[e] (ergs) | Mechanical Luminosity[e] ($L_\odot$) |
|---|---|---|---|---|---|---|---|
| Blue ..... | 11 | 0.20 | 1.8 $\times$ 10$^4$ | 0.10 | 0.6 | 3.6 $\times$ 10$^{43}$ | 0.02 |
| Red ..... | 14 | 0.43 | 3.0 $\times$ 10$^4$ | 0.08 | 0.5 | 4.0 $\times$ 10$^{43}$ | 0.01 |
| Total ..... | ... | ... | ... | 0.18 | 1.1 | 7.6 $\times$ 10$^{43}$ | 0.03 |

[a] Maximum velocity shift of the CO $J$ = 1–0 emission from $V_{LSR}$ = 2.7 km s$^{-1}$ at a 1 $\sigma$ level.
[b] The size was defined as maximum separation from the *IRAS* point source at the half-intensity level.
[c] Dynamical time scale was calculated by dividing the size of the outflow by $V_{max}$.
[d] Assumed the excitation temperature to be 30 K, and the optical depth of CO to be thin.
[e] Geometrical mean of upper and lower limits (Iwata, Fukui, & Ogawa 1988).

© American Astronomical Society • Provided by the NASA Astrophysics Data System

1992ApJ...392L..83U



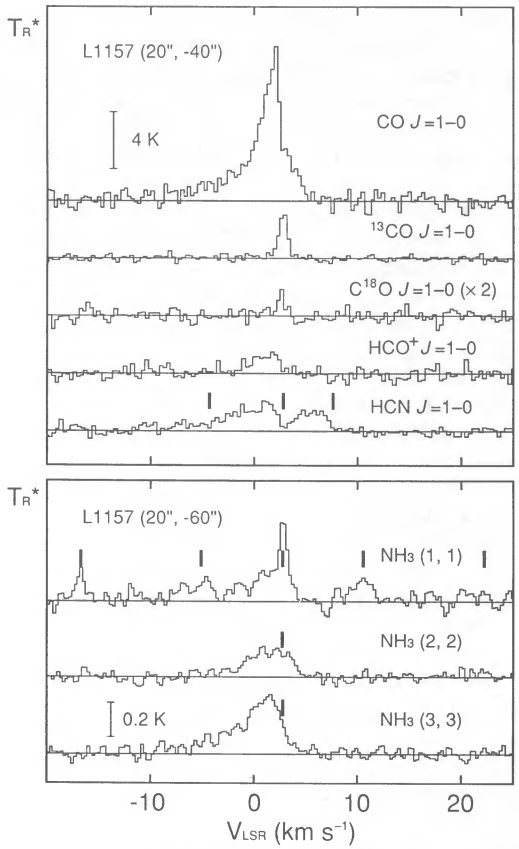


FIG. 2.—*Upper panel:* The CO, $^{13}$CO, C$^{18}$O, HCO$^+$, and HCN profiles averaged over $\sim$0.3 km s$^{-1}$ at ($\Delta$R.A., $\Delta$decl. = 20″, −40″), where the blue wing intensity is most prominent. *Lower panel:* The $NH_3$ profiles at (20″, −60″). The hyperfine components of HCN and $NH_3$ at the velocity of the quiescent cloud (2.7 km s$^{-1}$) are indicated by vertical heavy lines.

cides with that of the blue lobe of the outflow. It should be noted that the maximum position of CO intensity does not coincide with the *IRAS* source. Local intensity maxima are at the center and end of the blue lobe. We also note that the peak velocities of CO profiles are blueshifted in the blue lobe (see Fig. 2). Since the CO line in the blue lobe is not optically thick at the peak velocity, the excitation temperature of the CO gas should be higher than the observed radiation temperature (17 K). Thus the excitation temperature of CO gas in the blue lobe is higher than the value of $\leq$10 K for the ambient gas. These results suggest that the temperature rises in the outflowing CO gas of the blue lobe. This fact is remarkable, because previous CO observations indicated that the gas temperature of the outflows is equal to or lower than that of the ambient gas (e.g., Lada 1985). Such temperature enhancement was not observed toward the red lobe (Fig. 3).

In order to confirm the temperature enhancement in the blue lobe, we carried out the $NH_3$ observations, because the temperature derived from the rotation-inversion transition lines of $NH_3$ should be a good estimate of actual gas kinetic temperature. We estimated the rotational temperature from the intensity ratio of para-$NH_3$ (1, 1) and (2, 2) by following the method described in Ho & Townes (1983), and we assumed that the kinetic temperature is equal to the rotational temperature. We did not use the ortho-$NH_3$ (3, 3) data for the temperature determination, because the ortho-to-para ratio is unknown in this source. As shown in Figure 2, the $NH_3$ lines show significantly blueshifted wing emission in the blue lobe of the outflow. In the blue lobe of the outflow, the kinetic temperature averaged over the beam is derived to be 33 K for the blueshifted broad component. Although such high gas temperature is often observed in massive star-forming regions with luminous ($>10^4$ $L_\odot$) infrared sources (Takano 1986), it is rarely seen in low-mass star-forming regions.

The $NH_3$ lines at the *IRAS* position show only the narrow line shape without broad component. The brightness temperatures of the $NH_3$ (1, 1) and (2, 2) in the main component were 1.07 and 0.19 K, respectively, and the kinetic temperature was estimated to be 12 K. Thus the temperature does not rise significantly at the *IRAS* source position. We cannot state whether the temperature is enhanced in the red lobe because of the lack of $NH_3$ observations. However, the peak CO intensity seems to indicate that the gas temperature is not enhanced toward the red lobe. From these results, we can definitely conclude that the gas kinetic temperature considerably rises in the dense gas toward the blue lobe of the outflow, and that the temperature-enhanced region is apparently apart from the infrared source, even if uncertainty in the position of the *IRAS* source and the pointing error of the telescope are taken into account.

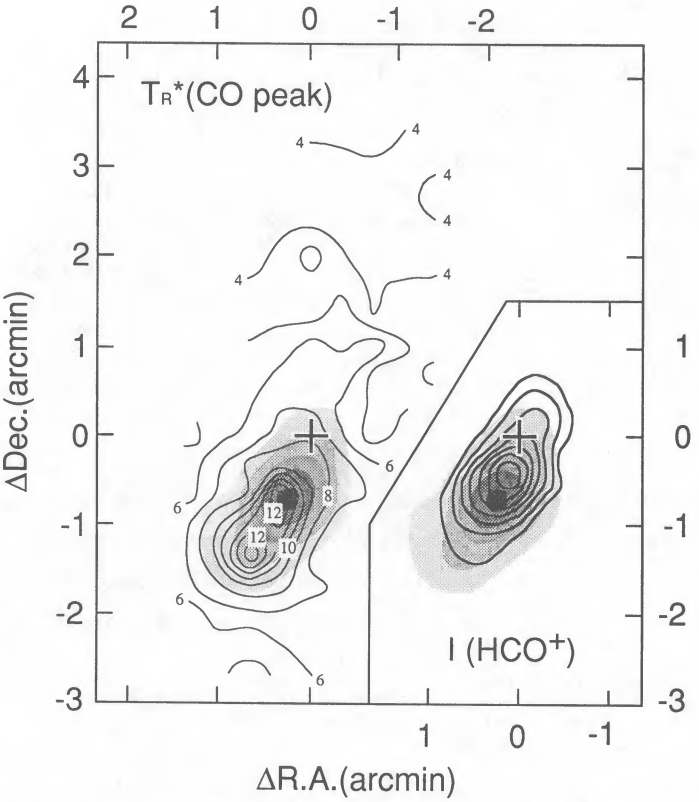


FIG. 3.—Contour maps of the peak CO radiation temperature (*thin line*) and the integrated intensity in HCO$^+$ over the range from −1 km s$^{-1}$ to 3 km s$^{-1}$ (*thick line*), superposed on the map of the CO blue lobe (*gray scale*). Contours for the CO are every 1 K from the lowest contour at 4 K. Contours for the HCO$^+$ are every 0.45 K km s$^{-1}$ from the lowest contour at 1.35 K km s$^{-1}$.

© American Astronomical Society • Provided by the NASA Astrophysics Data System

1992ApJ...392L..83U



## 4. DISCUSSION

The spatial coincidence between the temperature-enhanced region and the blue lobe of the outflow suggests that the temperature enhancement is physically related to the outflow phenomenon. The difference in spatial extent between blue and red lobe indicates that the ambient gas on the south side may obstruct the development of the blue lobe of the outflow, whereas the redshifted gas expanded out of the cloud toward the north rather freely. In fact, the temperature enhancement at the south side of the outflow suggests that the strong shock takes place there. The ambient gas, which was originally distributed toward the south of the *IRAS* source, seems to be compressed and accelerated by such strong shock to form the dense clumps observed by $HCO^+$ and HCN. Therefore we suggest that the gas is heated by the conversion of mechanical energy of the outflow into the thermal energy of the dense gas via shock. We can rule out a possibility of gas heating through collisions with the hot dust grains heated by radiation of the infrared source (Goldreich & Kwan 1974), because the temperature does not rise near the *IRAS* source.

It is worthwhile assessing whether the energy required for the temperature enhancement could be supplied by the mechanical energy of the outflow. The gas temperature may be determined by the thermal balance between the gas cooling by molecular line emission and gas heating by shock of the outflow. If the gas density, $n$, is $4 \times 10^5$ cm$^{-3}$ and the gas kinetic temperature, $T$, is 30 K, the molecular cooling rate, $\Lambda$, is estimated to be $2.1 \times 10^{-21}$ ergs cm$^{-3}$ s$^{-1}$, according to Goldsmith & Langer (1978). The total molecular line cooling luminosity within an extent of 0.08 pc $\times$ 0.13 pc (=the CS emitting region; Paper II) was estimated to be $\sim 9 \times 10^{-3}\ L_\odot$. This luminosity is smaller than the mechanical luminosity of the blueshifted gas of the outflow $\sim 0.02\ L_\odot$ (Table 1). This mechanical luminosity of the outflow can be regarded as a lower limit because of the following reasons. A small overlap of the red- and blueshifted CO emission indicates that an outflow axis is nearly perpendicular to our line of sight. In addition, the velocity extent of SiO $J = 2$–1 at the blue lobe is $\sim 20$ km s$^{-1}$, which is 2 times larger than that of CO, in high signal-to-noise ratio spectra (Paper II). The time scale listed in Table 1 is most likely overestimated. Therefore the mechanical luminosity of the outflow would be larger than the above estimate. Furthermore, the high-temperature dense gas may be in small clumps, as mentioned in § 3.2. If so, the volume of high-temperature gas and therefore the cooling luminosity are probably overestimated. On the basis of the above considerations, it seems that the cooling rate is much less than the heating rate. The temperature enhancement could be explained by the shock heating of the outflow, if a few percent of the mechanical energy of the outflow would be transferred to the thermal energy of the dense gas.

Next, we discuss why the temperature is prominently enhanced in the L1157 region. Fukui et al. (1989) suggested that molecular outflows associated with *IRAS* sources having significantly cold dust-color temperature may represent the main accretion phase of solar-type low-mass protostar evolution. IRAS 20386+6751 shows a cold far-infrared spectra (log $[F_\nu(25)/F_\nu(60)] = -1.57$, corresponding to a dust-color temperature of 46 K), and has no optical counterpart on the POSS prints. Judging from a short dynamical time scale of $< 10^4$ yr and the cold color temperature of the *IRAS* source, this object may be in the early stage in protostellar evolution. From the formula of Goldsmith & Langer (1978) $t_c = 3/2 \times kTn/\Lambda$, the gas cooling time scale, $t_c$, is estimated to be $\sim 4 \times 10^4$ yr, where $n = 4 \times 10^5$ cm$^{-3}$ and $T = 30$ K. This indicates that the gas cooling time scale is comparable to or slightly larger than the gas heating time scale (=the dynamical time scale of the outflow).

From the above discussions, we suggest that the L1157 outflow is so young that the ambient gas has not been blown out completely and that the shocked dense gas has not been cooled yet. Although the thermal influence by the outflow may be localized near the shock front, we can conclude that the molecular outflow has an influence on the parent cloud not only dynamically but also *thermally* via shock in its early evolutionary stage. The shock would also alter the chemical composition of the molecular gas in L1157 as indicated by the detection of SiO (Paper II). Because L1157 is a simple case of interstellar shock with little influence by radiation from the infrared source, our data will provide a better understanding of the shock physics and chemistry by comparing with the corresponding theoretical models.

The authors are grateful to K. Takakubo and K. Kawabata for their kind guidances and encouragements throughout this work. We thank K. Tatematu, A. Mizuno, & T. Nakano for their valuable discussions and critical reading of the manuscript. T. U. thanks the Japan Society for the Promotion of Science for financial support.

## REFERENCES

Clark, F. O., Laureijs, R. L., Chlewicki, G., Zhang, C. Y., van Oosterom, W., & Kester, D. 1986, A&A, 168, L1
Edwards, S., Strom, S. E., Snell, R. L., Jarrett, T. H., Beichman, C. A., & Strom, K. M. 1986, ApJ, 307, L65
Fukui, Y. 1989, in Low Mass Star Formation and Pre-main-Sequence Objects ed. B. Reipurth (Garching: ESO), 95
Fukui, Y., Iwata, T., Takaba, H., Mizuno, A., Ogawa, H., Kawabata, K., & Sugitani, K. 1989, Nature, 342, 161
Goldreich, P., & Kwan, J. 1974, ApJ, 189, 441
Goldsmith, P. F., & Langer, W. D. 1978, ApJ, 222, 881
Ho, P. T. P., & Townes, C. H. 1983, ARA&A, 21, 239
Iwata, T., Fukui, Y., & Ogawa, H. 1988, ApJ, 325, 372
Lada, C. J. 1985, ARA&A, 23, 267
Lane, A. P., & Bally, J. 1986, ApJ, 310, 820
Margulis, M., Lada, C. J., & Snell, R. L. 1988, ApJ, 333, 316
Margulis, M., Lada, C. J., & Young, E. T. 1989, ApJ, 345, 906
Mikami, H., Umemoto, T., Yamamoto, S., & Saito, S. 1992, ApJ, 392, L87 (Paper II)
Mizuno, A., Fukui, Y., Iwata, T., & Takano, T. 1990, ApJ, 356, 184
Myers, P. C., Heyer, M., Snell, R. L., & Goldsmith, P. F. 1988, ApJ, 324, 907
Takano, T. 1986, ApJ, 303, 349
Takano, T., Stutzki, J., Winnewisser, G., & Fukui, Y. 1985, A&A, 144, L20
Umemoto, T., Hirano, N., Kameya, O., Fukui, Y., Kuno, N., & Takakubo, K. 1991, ApJ, 377, 510
Viotti, N. R. 1969, Mem. Soc. Astron. Ital., 40, 75

© American Astronomical Society • Provided by the NASA Astrophysics Data System